Science Translational Medicine AAAS

Tryptophan Catabolism by Indoleamine 2,3-Dioxygenase 1 Alters the Balance of T_H17 to Regulatory T Cells in HIV Disease

David Favre, *et al.*

Sci Transl Med **2**, 32ra36 (2010);
DOI: 10.1126/scitranslmed.3000632

HIV/AIDS

Tryptophan Catabolism by Indoleamine 2,3-Dioxygenase 1 Alters the Balance of T_H17 to Regulatory T Cells in HIV Disease

David Favre,[1*†] Jeff Mold,[1*] Peter W. Hunt,[2] Bittoo Kanwar,[1,3] P'ng Loke,[1‡] Lillian Seu,[1] Jason D. Barbour,[2] Margaret M. Lowe,[1] Anura Jayawardene,[4] Francesca Aweeka,[4] Yong Huang,[5] Daniel C. Douek,[6] Jason M. Brenchley,[7] Jeffrey N. Martin,[8] Frederick M. Hecht,[2] Steven G. Deeks,[2] Joseph M. McCune[1§]

(Published 19 May 2010; Volume 2 Issue 32 32ra36)

The pathogenesis of human and simian immunodeficiency viruses is characterized by $CD4^+$ T cell depletion and chronic T cell activation, leading ultimately to AIDS. $CD4^+$ T helper (T_H) cells provide protective immunity and immune regulation through different immune cell functional subsets, including T_H1, T_H2, T regulatory (T_{reg}), and interleukin-17 (IL-17)–secreting T_H17 cells. Because IL-17 can enhance host defenses against microbial agents, thus maintaining the integrity of the mucosal barrier, loss of T_H17 cells may foster microbial translocation and sustained inflammation. Here, we study HIV-seropositive subjects and find that progressive disease is associated with the loss of T_H17 cells and a reciprocal increase in the fraction of the immunosuppressive T_{reg} cells both in peripheral blood and in rectosigmoid biopsies. The loss of T_H17/T_{reg} balance is associated with induction of indoleamine 2,3-dioxygenase 1 (IDO1) by myeloid antigen-presenting dendritic cells and with increased plasma concentration of microbial products. In vitro, the loss of T_H17/T_{reg} balance is mediated directly by the proximal tryptophan catabolite from IDO metabolism, 3-hydroxyanthranilic acid. We postulate that induction of IDO may represent a critical initiating event that results in inversion of the T_H17/T_{reg} balance and in the consequent maintenance of a chronic inflammatory state in progressive HIV disease.

INTRODUCTION

Accumulating evidence suggests that the pathology associated with HIV infection may result from persistent and uncontrolled inflammation (*1*). This hypothesis is supported by the observations that chronic, untreated HIV infection is associated with systemic immune activation, including increases in nonspecific T cell activation and proliferation (*2*), elevated inflammatory cytokines and chemokines (*3*), and increased concentration of catabolic by-products such as neopterin and kynurenine in the circulation (*4*). The central role of T cell activation and inflammation in HIV disease pathogenesis is supported by the consistent observation that activated ($CD8^+CD38^+HLA\text{-}DR^+$) circulating T cells predict disease progression independent of viral load (*5*). Other markers of inflammation [including interleukin-6 (IL-6) and high-sensitivity reactive protein] are also independent predictors of disease progression in both treated and untreated HIV infection (*6*).

Indoleamine 2,3-dioxygenase 1 (IDO1; previously referred as IDO or INDO) is the main inducible and rate-limiting enzyme for the catabolism of the amino acid tryptophan through the kynurenine pathway (*7*) (although there may be a separate and perhaps overlapping role for the newly discovered enzyme, IDO2) (*8*). Predominantly found in macrophages and dendritic cells (DCs), IDO1 is up-regulated by interferons (IFNs) and by agonists of Toll-like receptors (TLRs) (*7*). Increased catabolism of tryptophan by IDO1 suppresses T cell responses in a variety of diseases or states, including autoimmune disorders (*9*), allograft rejection (*10*), viral infections (*11*), cancer (*12*), and pregnancy (*13*). Such suppression is thought to occur either because IDO1 depletes the essential amino acid tryptophan or because it produces tryptophan catabolites that are toxic to T cells (or both) (*14*, *15*). In either case, the ability of IDO1 to suppress immune responses has raised the possibility that it may contribute to the immunodeficiency seen in individuals with progressive HIV disease (*4*).

Although $CD4^+$ T cell depletion is pathognomonic for HIV disease progression, the specific subsets of $CD4^+$ T helper (T_H) cells that are affected remain elusive. Four main lineages of $CD4^+$ T_H cells have been characterized, including IFN-γ–secreting T_H1 cells, IL-4–secreting T_H2 cells, FoxP3-expressing T regulatory (T_{reg}) cells, and IL-17–secreting T_H17 cells. These lineages derive from naïve $CD4^+$ T cells under polarizing and mutually exclusive conditions in vitro, and presumably in vivo (*16*), and provide protective immunity against intracellular (T_H1) or extracellular pathogens (T_H2) as well as immune regulation and tolerance (T_{reg}) or protection against bacterial infection at mucosal sites (T_H17) (*17*). We recently reported that simian immunodeficiency virus (SIV) infection leading to AIDS in macaques was associated with a change in the balance of T_{reg} and T_H17 cells, whereas this balance

[1]Division of Experimental Medicine, Department of Medicine, University of California, San Francisco, CA 94110, USA. [2]HIV/AIDS Program, Department of Medicine, University of California, San Francisco, CA 94110, USA. [3]Division of Gastroenterology, Department of Pediatrics, University of California, San Francisco, CA 94110, USA. [4]Drug Research Unit, Department of Clinical Pharmacy, University of California, San Francisco, CA 94143, USA. [5]Department of Bioengineering and Therapeutic Sciences, University of California, San Francisco, CA 94143, USA. [6]Human Immunology Section, Vaccine Research Center, National Institute of Allergy and Infectious Diseases, NIH, Bethesda, MD 20892, USA. [7]Laboratory of Molecular Microbiology, National Institute of Allergy and Infectious Diseases, NIH, Bethesda, MD 20892, USA. [8]Department of Epidemiology and Biostatistics, University of California, San Francisco, CA 94143, USA.
*These authors contributed equally to this work.
†Present address: National Immune Monitoring Laboratory, Montréal, Quebec H7N 4A4, Canada.
‡Present address: Department of Medical Parasitology, New York University, New York, NY 10010, USA.
§To whom correspondence should be addressed. E-mail: mike.mccune@ucsf.edu

was maintained in natural SIV infections that do not lead to AIDS in African green monkeys (*18*). T_H17 cells are also lost in HIV infection, which has been suggested to account for a breakdown in mucosal immunity and an increase in microbial translocation across the gastrointestinal mucosa (*19*). Despite the selective depletion of T_H17 cells during pathogenic SIV and HIV infection, there is no evidence that these cells are preferentially infected, and instead, bystander cell death may account for their loss (*19*). Studies in mice have suggested that IDO1 regulates the balance of T_H17 to T_{reg} cells, but the mechanism of such regulation remains unknown (*20*, *21*). We hypothesized that elevated IDO1 activity may alter the balance of T_H17 to T_{reg} cells after infection by HIV, thereby establishing a positive feedback loop that increases systemic immune activation and accelerates disease progression. Here, we extend previous studies to show that enhanced IDO1 activity is associated with HIV disease progression and demonstrate that such activity results in an imbalance of T_H17 and T_{reg} cells in the peripheral blood and in rectosigmoid tissue that is both linked to HIV disease progression and mediated by the tryptophan catabolite 3-hydroxyanthranilic acid (3-HAA).

RESULTS

IDO1 activity is elevated in progressive HIV infection

IDO1 activity measured in plasma is elevated in HIV-infected subjects compared to healthy controls, especially in those who have progressed to AIDS (*4*, *11*, *22*). We confirmed and expanded these findings in well-characterized cohort of HIV-infected subjects in varying stages of disease progression and treatment. Untreated HIV-infected subjects were stratified into three groups on the basis of viral load and $CD4^+$ T cell count at the time of the study: (i) controllers, defined as those with a steady-state viral load of <2000 HIV RNA copies per milliliter and a $CD4^+$ T cell count of >500 cells/μl (n = 20); (ii) noncontrollers/high CD4, with viral loads of >10,000 copies/ml and $CD4^+$ T cell counts of >350 cells/μl (n = 33); and (iii) noncontrollers/low CD4, with viral loads of >10,000 copies/ml and $CD4^+$ T cell counts of <350 cells/μl (n = 33) (for further details, see table S1 and Materials and Methods, Patient populations, Study A). Circulating concentrations of tryptophan were measured on plasma samples from each subject and found to be comparable in all groups (Fig. 1A, left). By contrast, kynurenine concentrations were significantly elevated in noncontrollers with low $CD4^+$ T cell counts as was the ratio of kynurenine to tryptophan (K/T ratio). When all 60 subjects were considered as a single group, kynurenine concentrations were positively correlated with viral load and with the amount of $CD4^+$ and $CD8^+$ T cell activation, as measured by the percentage of T cells expressing HLA-DR and CD38, and negatively associated with $CD4^+$ T cell counts (Fig. 1B).

Tryptophan and kynurenine concentrations were measured on a longitudinal basis within a subset of noncontrollers with high (n = 13) or low (n = 6) $CD4^+$ T cell counts [median interval between mea-

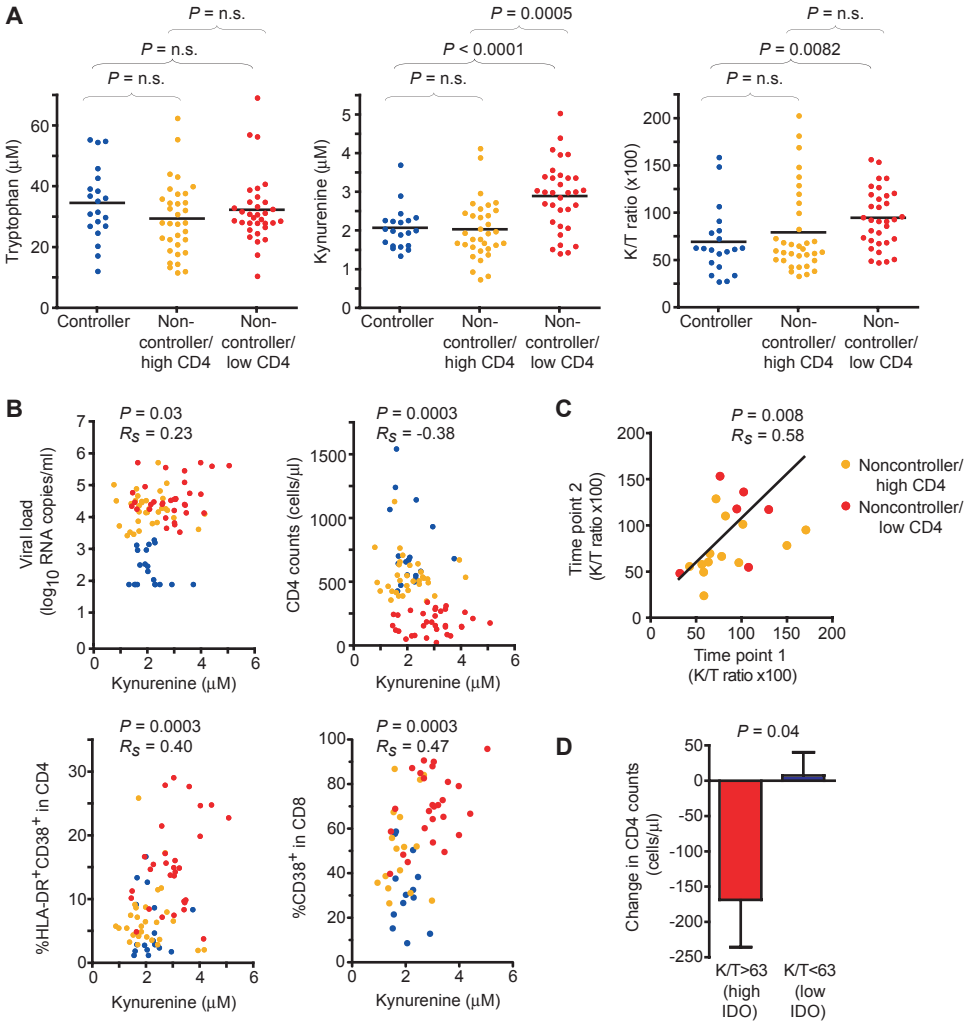

Fig.1. Tryptophan catabolism is elevated in HIV disease progression. Plasma samples were obtained from chronically HIV-infected subjects from the SCOPE Cohort, who were either viral controllers (n = 20) or noncontrollers with high or low $CD4^+$ T cell counts (respectively, higher or lower than 350 cells/μl, n = 33 in each group) (for further details, see Materials and Methods, Patient populations, Study A, and table S1). (**A**) Plasma concentration of circulating tryptophan (left), kynurenine (middle), and K/T ratio (right). n.s., not significant. (**B**) Correlation of plasma kynurenine concentration with measures of HIV disease progression, including viral load, $CD4^+$ T cell counts, as well as $CD4^+$ and $CD8^+$ T cell activation status, as measured by the fraction of cells positive for HLA-DR and CD38. The colors in these panels correspond to those in (A). (**C**) K/T ratio over time in noncontrollers with high or low $CD4^+$ T cell counts (median, 7.8 months; IQR, 4.7 to 11.9 months). (**D**) Change of $CD4^+$ T cell counts over time in viral noncontrollers with high $CD4^+$ T cell counts (>500 cells/μl) and either high or low K/T ratios (respectively, higher or lower than 63.2, the median K/T ratio from all noncontrollers). The Mann-Whitney U test was used for group comparisons. The Spearman rank correlation test was used for correlations, with R_s being the Spearman correlation coefficient.

surements, 7.8 months; interquartile range (IQR), 4.7 to 11.9; median K/T ratio = 63], and the K/T ratios were constant over time (Fig. 1C). Among noncontrollers with high $CD4^+$ T cell counts (>500 $CD4^+$ T cells/μl), those with high IDO1 activity as measured by a K/T ratio higher than the median value for noncontrollers (K/T > 63) at the first time point exhibited a greater subsequent decline in $CD4^+$ T cell counts than those with low IDO1 activity at baseline (Fig. 1D). Consistent with a previous report (*22*), this observation indicates that high IDO1 activity is predictive of HIV disease progression.

IDO1 is expressed in the peripheral lymph nodes and gastrointestinal lymphoid tissues of HIV-infected progressors

Despite evidence that IDO1 correlates with HIV disease progression, incomplete knowledge exists about which cells produce the enzyme during the course of lentiviral infection. SIV-infected macaques exhibit a rapid increase of IDO1-positive $CD4^+$ T cells in the lymph nodes (*23*). However, after HIV infection of human peripheral blood mononuclear cells (PBMCs) in vitro, IDO1 expression was up-regulated mostly in plasmacytoid DCs (pDCs) (*24*). In nonhuman primates, IDO1 expression is up-regulated during acute infection in blood, lymph nodes, and colon but only sustained at high concentrations during pathogenic infection (*18*, *25*). We examined biopsies of lymph node and of rectosigmoid biopsy tissue from HIV^- and HIV^+ donors to determine the tissue localization and cell types responsible for IDO1 production during chronic HIV infection. As determined by quantitative polymerase chain reaction (PCR), HIV-infected noncontrollers (with both high and low $CD4^+$ T cell counts) had significantly elevated IDO1 messenger RNA (mRNA) in rectosigmoid tissue compared to HIV-infected controllers (Fig. 2A). Immunohistochemical analysis of lymph node and rectosigmoid tissue from HIV-infected noncontrollers (with both high and low CD4) showed prominent IDO1 staining within cells with a dendritic morphology in both tissues as compared to healthy HIV-seronegative controls or HIV-infected controllers (Fig. 2B, top panels). Immunofluorescent analysis revealed that many of the IDO1-positive cells expressed the myeloid DC marker DEC205 but that they did not express markers for T cells (CD3), the monocytic lineage (CD68), or pDCs (BDCA2) (Fig. 2B, bottom panels, and fig. S1). Thus, the myeloid antigen-presenting DC (mDC) population appears to contain a substantial fraction of the resident antigen-presenting cells in which IDO1 activity is up-regulated both in peripheral lymph nodes and in rectosigmoid biopsy tissue.

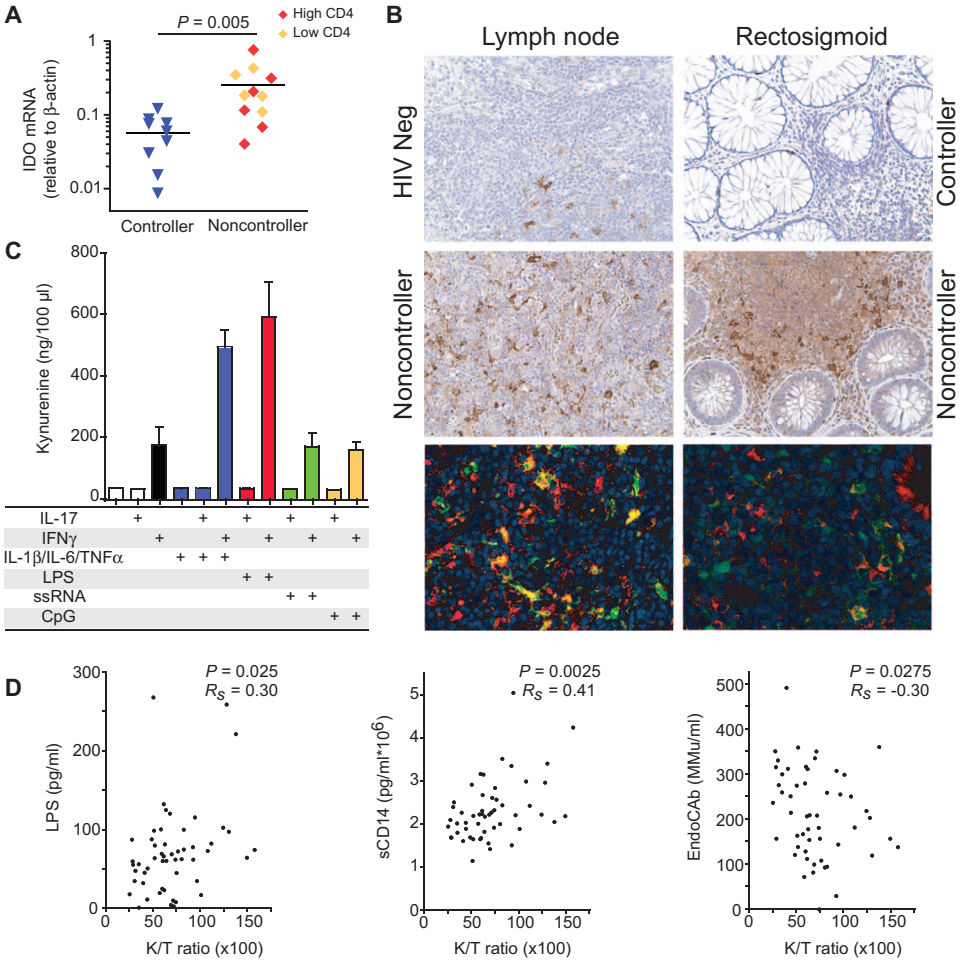

Fig. 2. IDO is up-regulated in mDCs in tissues from HIV^+ subjects and by IFN and LPS in vitro. (**A**) mRNA expression of IDO relative to that of β-actin in rectosigmoid biopsies from noncontrollers compared to controllers. (**B**) Top two rows: IDO expression by immunohistochemistry in lymph node (left panels) and in rectosigmoid biopsy tissues (right panels) of HIV-seronegative (HIV Neg) subjects or viral controllers compared to viral noncontrollers. Bottom row: Colocalization of IDO (green) and the mDC marker (DEC205) (red), visualized as cells that are yellow-orange in color (see arrows) in lymph node and rectosigmoid biopsy tissues. (**C**) IDO activity as measured by kynurenine concentration in the supernatant of monocyte-derived DCs after exposure to IFN-γ alone and in combination with LPS or other TLR ligands, as well as with inflammatory cytokines IL-17 or a mix of IL-1β, IL-6, and TNFα. Data are representative of that measured in two donors. (**D**) Correlation between K/T ratio and plasma concentrations of LPS (left), sCD14 (middle), and EndoCAb concentrations (right). The Mann-Whitney *U* test was used for group comparisons. The Spearman rank correlation test was used for correlations, with R_s being the Spearman correlation coefficient. MMu, immunoglobulin M median units.

IDO1 activity in mDCs is activated by IFN-γ and enhanced by LPS

Both mDCs and pDCs are important in regulating immune responses; each population, however, exhibits distinct requirements for activation. Thus, pDCs show up-regulation of IDO1 after direct engagement of CD4 with gp120 or after stimulation with IFNs or TLR7/9 agonists (*24*, *26*). On the other hand, mDCs are more responsive to bacterial components, including lipopolysaccharide (LPS), which signals through

TLR4 (*27*). Recent studies have demonstrated elevated LPS concentrations in peripheral blood during chronic HIV infection, linking bacterial translocation from the gut to systemic immune activation and disease progression (*28*).

To determine which signaling pathways might be involved in the activation of IDO1, we generated mDCs from peripheral blood monocytes of healthy donors, stimulated under varying conditions, and then assayed for the production of kynurenine (Fig. 2C and fig. S2). IFN-γ, but not IL-17, was found to promote IDO1 activity as assessed by kynurenine measurement in cultured mDCs. Activation by the inflammatory cytokines IL-1β, IL-6, and tumor necrosis factor α (TNFα) enhanced the ability of IFN-γ to promote IDO1 activity but did not promote IDO1 activity alone. As reported for LPS alone (*29–31*), LPS plus IL-17 (Fig. 2C) or in combination with IL-1β, IL-6, and TNFα (fig. S2) did not promote IDO1 activity; LPS in combination with IFN-γ, however, did enhance IDO1 activity (Fig. 2C), as it did in combination with IFN-γ plus IL-1β, IL-6, and TNFα (fig. S2). Meanwhile, single-stranded RNA (ssRNA) (a TLR7 agonist) or CpG (a TLR9 agonist) had no apparent effect on IDO1 activity alone or in synergy with IFN-γ alone (Fig. 2C) or with IFN-γ in combination with IL-1β, IL-6, and TNFα (fig. S2).

We next investigated whether IDO1 activity in chronically infected HIV-positive subjects was associated with elevated LPS concentrations in peripheral blood. A significant positive correlation was found between IDO1 activity (as measured by K/T ratios) and plasma LPS concentrations in HIV-infected subjects (Fig. 2D, left panel). Likewise, a significant positive correlation was observed between IDO1 activity and plasma concentrations of soluble CD14 (sCD14), which increases in relation to LPS concentrations (Fig. 2D, middle panel) (*28*). Finally, a negative correlation was observed between IDO1 activity and circulating concentrations of endotoxin core antibodies (EndoCAb), which bind to and are known to decrease in the presence of elevated concentrations of LPS (Fig. 2D, right panel) (*28*). Together, these data suggest that elevated LPS concentrations associated with microbial translocation into the bloodstream may augment IDO1 activity in HIV-infected subjects by stimulating TLR4 on mDCs.

A decreased T_H17/T_{reg} ratio is linked to HIV disease progression

Depletion of gut mucosal $CD4^+$ T cells during pathogenic lentiviral infection is thought to lead to microbial translocation across the mucosal barrier and increases in the circulating concentrations of LPS (*32*). However, T cell loss in the gastrointestinal mucosa also occurs in nonpathogenic SIV infection without microbial translocation (*33*). We and others have shown that T_H17 cells are selectively depleted in pathogenic SIV and HIV infection but maintained in nonpathogenic infections (*18*, *19*). T_H17 cells are important in controlling bacterial growth in mucosal tissues, and loss of T_H17 cells in pathogenic SIV infection correlates with increased microbial translocation to peritoneal draining lymph nodes and the peripheral blood and lymphatic systems (*34*).

Despite strong evidence that a loss of T_H17 cells is characteristic of pathogenic SIV and HIV infection, the underlying mechanisms accounting for the selective depletion of T_H17 cells remain unclear. A clue to a potential mechanism for T_H17 cell depletion was suggested by the observation that their loss in pathogenic SIV infection was accompanied by a concomitant rise in the frequency of induced T_{reg} cells (*18*). Thus, although they perform substantially different roles during the course of an immune response, T_H17 and T_{reg} cells have reciprocal differentiation pathways from a common T cell progenitor (*35–38*). Given this relation, we analyzed the frequency of T_H17 (IL-17A–secreting) cells and T_{reg} ($FoxP3^+$) cells among $CD4^+$ T cells in PBMCs and rectosigmoid biopsy tissue from HIV-negative and HIV-infected subjects, including, as in the aforementioned Study A, viral controllers and noncontrollers, and those whose virus was suppressed as a result of long-term antiretroviral therapy (see Materials and Methods, Patient populations, Studies B and C, for further details on these cohorts). More than 95% of the $CD4^+$ T cells from rectosigmoid tissue displayed a memory phenotype ($CD45RA^-CD27^{+/-}$), whereas only a fraction of peripheral blood $CD4^+$ T cells had such a phenotype (fig. S3, A and B). Almost all T_H17 cells also had a memory phenotype ($CD45RA^-CD27^{+/-}$) (fig. S3C) and produced IL-17A as well as significant amounts of IL-2, IL-22, and TNFα. The T_H17 cells were substantially more frequent in $CD4^+$ T cells from rectosigmoid biopsy tissue than in peripheral blood (about eight times higher in the representative example shown in Fig. 3A). Because the proportion of memory $CD4^+$ T cells in the peripheral blood was different from that in the rectosigmoid biopsies, we measured the frequency of T_H17 cells within the memory $CD4^+$ T cell fraction in PBMCs. In peripheral blood, noncontrollers with more advanced disease (with CD4 of <350 cells/μl) showed a decreased proportion of memory T_H17 cells than did HIV-negative subjects (Fig. 3B, top panel) and an increased proportion of memory $FoxP3^+$ T_{reg} cells compared to controllers, HIV-positive subjects with suppressed viral loads, and HIV-negative subjects (Fig. 3B, bottom panel). When the frequencies of these subpopulations were compared to one another, the T_H17/T_{reg} ratio was about 5 and 10 times lower in noncontrollers with advanced CD4 depletion when compared to noncontrollers with preserved CD4 counts and HIV-negative individuals, respectively (Fig. 3C). The T_H17/T_{reg} ratio was inversely related to $CD8^+$ T cell activation (as measured by CD38 and Ki67 expression in $CD8^+$ T cells) (Fig. 3D). Notably, the T_H17/T_{reg} ratio was also decreased among the antiretroviral-treated subset with undetectable viral loads, a result that was largely driven by five subjects whose T_H17/T_{reg} ratio did not return after treatment to a point comparable to that of HIV-negative individuals or viral controllers.

To determine the relation between T_H17 cells and immune activation at early stages of HIV infection (during the first year), were studied PBMCs from 27 subjects 3 months (acute) and 12 months (chronic) after the estimated date of HIV infection (see Materials and Methods, Patient populations, Study C, and table S1). We determined the difference in T cell immune activation between these two time points ($\Delta Ki67^+$ in $CD8^+$ T cells) and calculated independent predictors of decreased or increased T cell immune activation with a multivariate mixed-effects analysis. Independent covariates included memory T_H17 cells, $CD4^+$ T cell counts, and $\log_{10}$-transformed plasma viral load during acute infection. We found that a higher frequency of memory T_H17 cells during acute infection (3 months) was a predictor of decreased T cell immune activation over time (−4.56 lower $CD8^+Ki67\%$ per each 1 percentage point higher of $CD4^+T_H17\%$, $P = 0.0098$), independent of $CD4^+$ T cell counts and viral load.

This relation was further analyzed in three groups defined by low or high viral load and immune activation (CD38 expression in $CD8^+$ T cells) at 12 months (a time when viral and immunological set points are established). These groups were defined in the following manner: Group 1 with low viral load and low immune activation, Group 2 with high viral load and high immune activation, and Group 3 with high viral load but low immune activation (Fig. 3E, left). Previous results

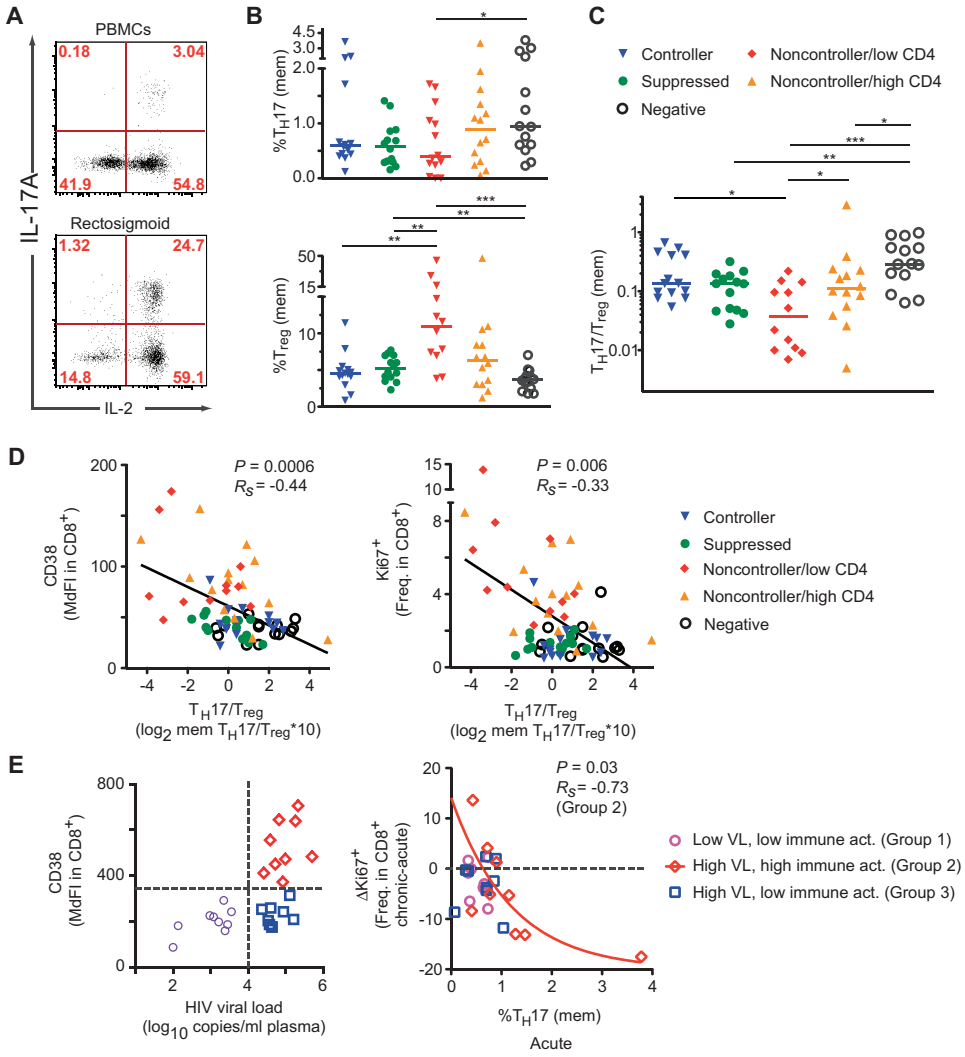

Fig. 3. Loss of T_H17 cells and inversion of T_H17/T_{reg} ratio is related to immune activation and HIV disease progression in peripheral blood. A cross-sectional analysis was carried out on PBMCs from HIV-negative and HIV-infected subjects from the SCOPE Cohort who were controllers (blue triangles), suppressed (green circles), noncontrollers/low CD4 (red diamonds), noncontrollers/high CD4 (yellow triangles), or HIV-seronegative (black circles) (n = 14 in each group) (for further details, see Materials and Methods, Patient populations, Study B, and table S1). In addition, a longitudinal analysis was performed on PBMCs from 27 subjects from the Options Cohort collected at ~3 months (acute) and ~12 months (chronic) after HIV infection. These subjects were divided into three groups (of nine subjects each) on the basis of plasma viral load and T cell immune activation at the second time point: Group 1 with low viral load and low immune activation (purple circles), Group 2 with high viral load and high immune activation (red diamonds), and Group 3 with high viral load and low immune activation (blue squares) (for further details, see Materials and Methods, Patient populations, Study C). Memory ($CD45RA^-CD27^{+/-}$) IL-17A–expressing T_H17 cells and $FoxP3^+$ T_{reg} cells were enumerated as described in Materials and Methods. (**A**) Example of intracellular FACS detection of IL-17A– and IL-2–expressing $CD4^+$ T cells after PMA-ionomycin stimulation on total PBMCs (top panel) and on cells from rectosigmoid biopsies (bottom panel) from the same HIV controller. (**B**) Frequencies of memory (mem) T_H17 cells (top panel) and T_{reg} cells (bottom panel) in patient groups. (**C**) T_H17/T_{reg} ratio in patient groups. (**D**) Correlation between T_H17/T_{reg} ratio (expressed as $\log_2$ memory T_H17/T_{reg} cells × 10) with systemic T cell immune activation, as measured by CD38 (left) and Ki67 expression (right) on peripheral blood $CD8^+$ T cells. (**E**) Viral load and immune activation set points at 12 months after primary HIV infection (left) delineate three groups with either low viral load and low immune activation (Group 1, purple circles), high viral load and high immune activation (Group 2, red diamonds), or high viral load but low immune activation (Group 3, blue squares). Correlation between the frequency of memory T_H17 cells during acute infection (3 months after infection) and the change of T cell immune activation between acute to chronic infection, as measured (difference of $Ki67^+$ in $CD8^+$ T cells from 3 to 12 months after infection) (right). Mann-Whitney U test was used for group comparisons (*$P < 0.05$, **$P < 0.005$, ***$P < 0.0005$). The Spearman rank correlation test was used for the correlations, with R_s being the Spearman correlation coefficient. The correlation (red curve) with P values and R_s in (E) is indicated for Group 2.

(5) have shown that viral load and immune activation are independent predictors of rapid HIV disease progression and, predictably, subjects in Group 2 had more rapid increases in viral load and decreases in $CD4^+$ T cell counts than did subjects in Groups 1 and 3 in the absence of antiretroviral treatment. Regression analysis revealed that a higher frequency of T_H17 cells at 3 months was correlated with a larger reduction of T cell immune activation ($\Delta Ki67^+$ in $CD8^+$ T cells) in subjects with more rapidly progressing HIV disease (Group 2, P = 0.03, R_s = –0.73) (Fig. 3E, right). As has been reported in SIV-infected, nonhuman primates (*18*), these results support the notion that a larger pool of T_H17 cells during acute infection correlates with better resolution of immune activation during progressive HIV disease.

Given the critical role of T_H17 cells in maintaining host barriers and immune surveillance at mucosal sites, the frequency of T_H17 and T_{reg} cells was also examined in rectosigmoid biopsy tissue from 9 controllers and 11 noncontrollers (see Materials and Methods, Patient populations, Study D). Similar to the situation in peripheral blood, the frequency of T_H17 cells (expressing IL-17A as well IL-2, IL-22, and TNFα) was lower, and the frequency of T_{reg} cells (expressing FoxP3 and Ki67) was higher, in noncontrollers than in the controllers (Fig. 4, A and B), resulting in a lower T_H17/T_{reg} ratio in the former group of subjects with more advanced disease (Fig. 4C). This ratio was inversely related to $CD8^+$ T cell activation (Fig. 4D) and to circulating 16*S* ribosomal DNA (rDNA) (Fig. 4E). Thus, as

in the case of nonhuman primate lentiviral infection (*18*, *34*), the degree of microbial translocation and T cell activation in progressive HIV disease is tightly associated with skewed maturation along the T_H17/T_{reg} axis.

Tryptophan catabolites directly influence T_H17/T_{reg} cell ratios

Tryptophan catabolism through the IDO1 pathway can regulate the balance between T_H17 cells and other T cell subsets, including T_{reg} cells (*20*, *21*). In HIV infection, pDCs influence T_{reg} frequencies in an IDO1-dependent fashion, but the mechanism underlying the generation of T_{reg} cells is unclear (*39*). Treatment of mice with L-kynurenine influenced the ratio of T_H17 and T_{reg} cells in vivo (*21*). This effect was inhibited by a kynurenine-3-monooxygenase inhibitor, suggesting that tryptophan catabolites downstream of kynurenine are likely to be involved in controlling the T_H17/T_{reg} cell balance (*21*).

To address the role of different tryptophan catabolites in human T cell differentiation, we performed activation assays in vitro on human T cells from normal and HIV-infected patients in the presence of varying concentrations of the tryptophan catabolites: 3-hydroxykynurenic acid (3-HKA), 3-HAA, and picolinic acid (PA) (Fig. 5A). Notably, tryptophan catabolites such as quinolinic acid have been linked to the neurological defects associated with HIV infection but not to the regulation of immune function (*40*). By contrast, 3-HKA and 3-HAA have both been shown to influence T cell activation (*10*, *15*, *21*, *41*). We noted a significant decrease in IL-17A–producing cells in the presence of both 3-HAA and 3-HKA but not in the presence of PA. Such decreases occurred primarily in T_H17 cells that were IFN-γ–negative and were dose-dependent with increasing concentrations of catabolites, most notably 3-HAA (Fig. 5B and fig. S4A). We also determined the ability of different tryptophan catabolites to promote the differentiation of $FoxP3^+$ T_{reg} cells. Only 3-HAA enhanced the proportion of $CD4^+CD25^+$ T cells expressing FoxP3, an effect that also occurred in a dose-dependent manner (Fig. 5C). No dose-dependent change in IFN-γ production (Fig. 5D, left panel) or in cell proliferation, as assessed by carboxyfluorescein succinimidyl ester (CFSE) dilution (Fig. 5D, right panel), was observed within the $CD4^+$ T cell population. Finally, we performed the same assay on PBMCs from HIV-infected controllers (n = 4) and found similar dose-dependent T_H17 depletion by tryptophan catabolites (fig. S4B).

To determine whether tryptophan catabolism has a similar effect in vivo, we related the presence and function of IDO1 to HIV disease progression. In rectosigmoid tissue from controllers (n = 9) and noncontrollers (n = 11) (Study Group D), IDO1 mRNA expression was inversely related to the T_H17/T_{reg} ratio (Fig. 5E). When analyzed in plasma, a similar relation was found between higher IDO1 activity (as measured by K/T ratio) and low T_H17/T_{reg} ratios (Fig. 5F). These observations support the hypothesis that IDO1-mediated tryptophan catabolism plays a critical role in determining T cell differentiation pathways during HIV infection and, thus, permit microbial translocation that drives disease progression.

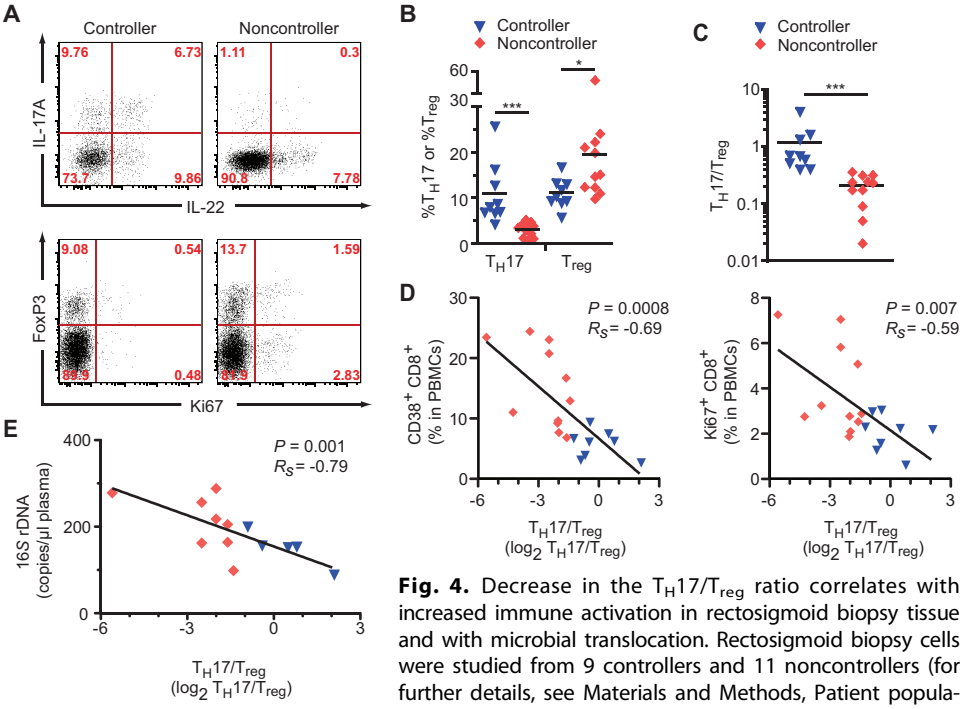

Fig. 4. Decrease in the T_H17/T_{reg} ratio correlates with increased immune activation in rectosigmoid biopsy tissue and with microbial translocation. Rectosigmoid biopsy cells were studied from 9 controllers and 11 noncontrollers (for further details, see Materials and Methods, Patient populations, Study D, and table S1). (**A**) Example of intracellular FACS detection of IL-17A and IL-22 (top panels) and of FoxP3 and Ki67 (bottom panels) in $CD4^+$ T cells from rectosigmoid biopsies in representative examples of viral controller and noncontroller subjects. (**B**) Frequency of T_H17 and $FoxP3^+$ T_{reg} cells in rectosigmoid biopsies from noncontrollers compared to controllers. (**C**) T_H17/T_{reg} ratio in patient groups. (**D**) Correlation between T_H17/T_{reg} ratio in rectosigmoid biopsies (expressed as $\log_2 T_H17/T_{reg}$) and systemic T cell activation as measured by CD38 and Ki67 expression in $CD8^+$ T cell from paired PBMCs. (**E**) Plasma concentration of 16*S* rDNA (a marker of bacterial translocation) in samples within the linear range of detection. Mann-Whitney *U* test was used for group comparisons (*P < 0.05, **P < 0.005, ***P < 0.0005). The Spearman rank correlation test was used for the correlations (R_s, Spearman correlation coefficient).

DISCUSSION

Research on aberrant immune system features in host-pathogen interactions, on inflammatory syndromes and autoimmune diseases, and on primary immune deficiencies has highlighted the importance of two immune cell lineages derived from a common progenitor under reciprocal and mutually exclusive differentiation pathways (*35*–*38*): T_H17 cells, which produce the proinflammatory cytokine IL-17, and $FoxP3^+$ T_{reg} cells, whose function is immunosuppressive (*42*–*45*). T_H17 cells, in particular, have been causally related both to chronic inflammatory diseases (*46*) and to host defenses against microbial agents (*47*). An intriguing developmental link also exists between the activity of the enzyme IDO1 and the differentiation of T_H17 and T_{reg} cells from naïve T cells. The products of IDO1, tryptophan catabolites such as kynurenines, can induce FoxP3 expression and the generation of T_{reg} cells and can blunt the generation

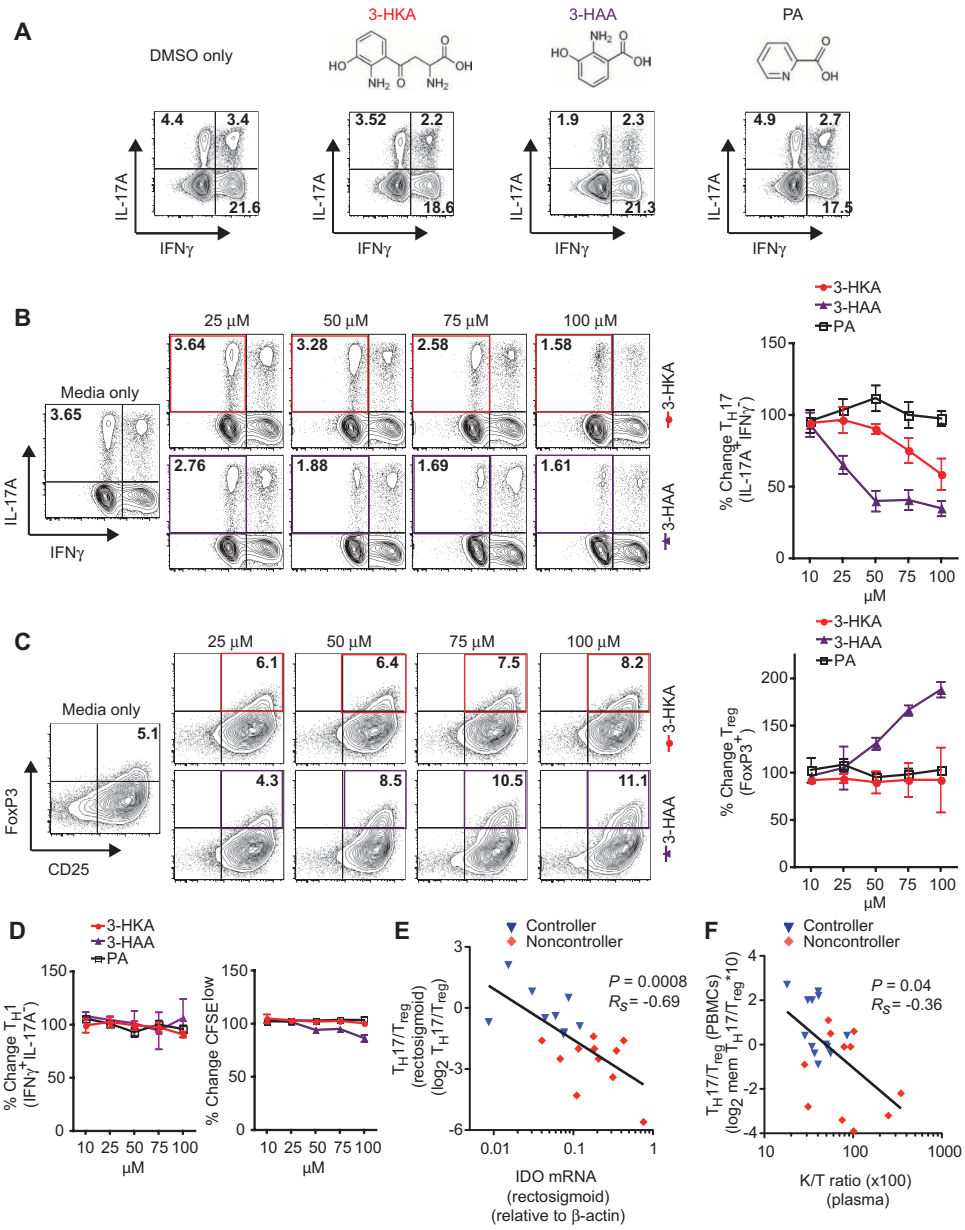

Fig. 5. IDO catabolites affect the T_H17/T_{reg} ratio. PBMCs from healthy donors were cultured in vitro for 6 days in the presence of different IDO catabolites, including 3-HKA, 3-HAA, and PA. (**A**) Formulae of the IDO catabolites 3-HKA, 3-HAA, and PA and example of intracellular FACS detection of IL-17A and IFN-γ expression in $CD4^+$ T cells after cell division ($CFSE^{low}$) for 3-HKA, 3-HAA, and PA compared to media. DMSO, dimethyl sulfoxide. (**B**) Frequency of IL-$17A^+$IFN-γ^- $CD4^+$ T cells after treatment with escalating doses of 3-HKA, 3-HAA, and PA. FACS results from one donor after 3-HKA and 3-HAA treatment are shown in the left panels. Results from four independent experiments with four different donors are at the right panel and show the normalized, mean percent change in T_H17 cells (corresponding to the ratio between the frequency of IL-$17A^+$IFN-γ^- T_H17 cells after treatment with IDO catabolites and the frequency of T_H17 cells treated with control vehicle and media alone). (**C**) Dose-dependent changes in $FoxP3^+$ T_{reg} cells in the same experiments and example as in (B). (**D**) Dose-dependent changes in T_H1 (IL-$17A^-$IFN-γ^+ $CD4^+$ T cells) and in proliferation ($CFSE^{low}$). (**E**) Correlation between the T_H17/T_{reg} ratio and IDO mRNA expression in rectosigmoid biopsy tissues from HIV controller and noncontroller subjects (Cohort Study D). (**F**) Correlation between the T_H17/T_{reg} ratio in PBMCs and K/T ratio in plasma from HIV controller and noncontroller subjects (Cohort Study B). The Spearman rank correlation test was used for the correlations (R_s, Spearman correlation coefficient).

of T_H17 cells and the expression of the master regulator of T_H17 differentiation, the RORc gene transcription factor (retinoic acid receptor–related orphan receptor-γt) (*20*, *21*, *48*). Similarly, IDO1-mediated tryptophan deprivation and the amino acid starvation response can induce T_{reg} development and blunt T_H17 conversion (*49*, *50*). Because IDO1 metabolism is related both to this T_{reg} to T_H17 developmental switch and to HIV pathogenesis (*4*), we explored the relations between HIV disease, T_H17 and T_{reg} cell populations, and IDO1 metabolism. We have demonstrated here that the balance between T_H17 and T_{reg} cells in blood and in the rectosigmoid mucosa is altered during HIV disease progression toward a lower proportion of T_H17 cells and an increased proportion of T_{reg} cells and that this change is directly associated with IDO1 activity. We also demonstrate that 3-HAA, a proximal catabolite of tryptophan catabolism, is capable of tipping the T_H17/T_{reg} balance toward the immunosuppressive T_{reg} pathway in vitro.

The deleterious nature of chronic inflammation has long been recognized in situations where the immune system fails to effectively clear pathogenic organisms (*51*). Certain strains of lymphocytic choriomeningitis virus (LCMV), for instance, can establish a chronic infection that eventually results in exhaustion of the immune system (*51*). More than 50 years ago, however, it was noted that vertical transmission of LCMV from mother to child results in chronic infection in the absence of overt pathology (*52*), a result of a failure of the immune system to attack LCMV (*52*, *53*). A similar situation occurs in nonpathogenic SIV infection in most African nonhuman primates (*54*). These animals maintain high viral loads in the absence of disease progression with reduced inflammatory responses during the chronic phase of the infection (*18*, *54*). Thus, disease associated with chronic infections such as HIV may not be so much a result of the virus attacking the host but rather may be a result of the host's immune system attacking the virus. In this regard, IDO1 may be one of many mediators through which an activated immune system and inflammation lead to a loss of T cell function and, ultimately, immunosuppression.

We propose here the existence of a feedback loop that leads to elevated sys-

temic immune activation during pathogenic HIV infection (*44*). We hypothesize that systemic inflammation in the acute stage of HIV infection, combined with the early loss of immune function caused by T_H17 cell depletion in the gastrointestinal tract, results in elevated IDO1 activity throughout the chronic phase of HIV infection. Such elevated activity, in turn, leads to the generation of catabolites (3-HAA) that alter T cell differentiation pathways in a manner that leads to further immunosuppression. Previous reports indicate that acute HIV and SIV infections result in a massive increase in IFN concentrations in part through direct activation of pDCs by HIV virions (*24*, *25*). Activated pDCs are then prompted to up-regulate IDO1 through autocrine IFN signaling and TLR stimulation by HIV components (for example, ssRNA or CpG) (*26*). The early burst of IDO1 activity results in a transient alteration in the T cell response favoring the up-regulation of FoxP3 and generation of T_{reg} cells over the differentiation of T_H17 cells. In nonpathogenic SIV infection, the IFN response is eventually curtailed and IDO1 activity returns to baseline levels (*18*). However, in pathogenic SIV infection and chronic HIV infection, IFN remains high, leading to the persistence of elevated IDO1 activity, likely from both pDCs and, on the basis of our data here, mDCs as well (*18*, *25*). This chronic activation of the IDO1 pathway diminishes the host's capacity to generate T_H17 cells and favors the generation of T_{reg} cells. The net outcome is a progressive loss of the mucosal immune barrier and increased susceptibility to mucosal infections, a result of fewer T_H17 cells, augmented by more T_{reg} cells, which dampens T cell immunity to HIV and other pathogenic organisms (*44*).

Although we have demonstrated that 3-HAA can specifically invert the ratio of T_H17 and T_{reg} cells, we have yet to determine the mechanism by which this occurs. Previous studies have shown that 3-HAA blocks T cell activation and promotes T cell death (*15*, *41*). These studies generally used higher concentrations of 3-HAA than reported here (and we have also observed cellular toxicity at concentrations >100 mM). 3-HAA has also been found to inhibit T_H1 and T_H2 responses in a variety of in vivo settings, including allergy (*55*), organ transplantation (*10*), experimental autoimmune encephalomyelitis (*9*), and colitis (*56*). One study has shown that 3-HAA mediates its inhibitory effects on T cell activation and proliferation by directly inhibiting the phosphorylation of phosphoinositide-dependent kinase 1 and by preventing nuclear factor κB activation after T cell receptor stimulation (*57*). However, we did not observe increases in T cell death or inhibition of proliferation at lower concentrations of 3-HAA (25 to 100 mM) despite alterations in T_H17 and T_{reg} cell differentiation.

IDO1-dependent tryptophan catabolism may be an important link between immune activation and the gradual decline of immune function seen in progressive HIV infection. Blockade of IDO1 with a pharmacological inhibitor (for example, 1-methy-D-tryptophan) in combination with antiretroviral therapy has shown some promise in lowering the viral load in pathogenic SIV infection (*58*) and enhancing the elimination of virus-infected macrophages in a murine model of HIV encephalitis (*59*). Clinical trials are currently under way to assess the efficacy of IDO1 inhibitors for cancer immunotherapy, and small-molecule inhibitors are being developed that may prove useful in a variety of clinical settings. Future efforts to determine whether blockade of IDO1 can alter the balance of T cell subsets in disease states represent an important goal for understanding HIV pathogenesis as well as other diseases characterized by chronic inflammation.

MATERIALS AND METHODS

Patient populations

PBMCs, plasma, and rectosigmoid biopsies were obtained from HIV-infected adults enrolled in the University of California, San Francisco (UCSF) SCOPE Cohort or the UCSF Options Cohort (*5*). SCOPE is an ongoing prospective cohort study aimed at investigating the long-term clinical and immunological consequences of HIV infections and their treatment. The UCSF Options Cohort is an early HIV infection cohort in which participants are enrolled within 12 months of HIV antibody seroconversion (typically within 6 months of seroconversion). Subjects were determined to be in early HIV infection via an algorithm using information on serial HIV antibody testing, less sensitive enzyme immunoassay antibody testing, RNA PCR detection, HIV protein Western blot banding patterns, and self-reported risk behaviors to estimate time since infection. All participants gave written informed consent using protocols approved by the Committee on Human Research, UCSF.

Four separate studies of HIV-infected subjects from SCOPE and Options Cohorts contributed to this analysis.

Study A. For the measurements of tryptophan and kynurenine shown in Figs. 1 and 2D, plasma was obtained from subjects in the SCOPE Cohort who were either (i) controllers, defined as those with a steady-state viral load of <2000 copies/ml and a $CD4^+$ T cell count of >500 cells/μl (n = 20); (*2*) noncontrollers/high CD4, with viral loads of >10,000 copies/ml and $CD4^+$ T cell counts of >350 cells/μl (n = 33); or (*3*) noncontrollers/low CD4, with viral loads of >10,000 copies/ml and $CD4^+$ T cell counts of <350 cells/μl (n = 33). As per the SCOPE protocol, these subjects had contemporaneous viral loads, $CD4^+$ T cell counts, and measurements of $CD4^+$ and $CD8^+$ T cell activation. Some of these plasma specimens had also previously been analyzed for endotoxin (LPS), sCD14, and EndoCAb (*28*).

Study B. For immunophenotyping and measurement of T_H17 and T_{reg} cells in the peripheral blood of chronically infected subjects (Fig. 3), cryopreserved PBMCs were obtained from untreated subjects in the SCOPE Cohort who were controllers (n = 14) or noncontrollers (n = 28). As above in Study A, controllers were defined by undetectable or low plasma RNA HIV viral load (<2000 copies/ml) (median, <75; IQR, <75 to <75) and $CD4^+$ T cell counts of >500 cells/μl of blood (median, 814; IQR, 713 to 1156). Noncontrollers were defined by a viral load of >10,000 copies/ml, with evidence of progressive disease (CD4 decline over time >50 cells per year), and further subdivided in groups with high or low CD4 counts [for example, CD4 counts of >350 cells/μl (median, 504; IQR, 473 to 541) or <350 cells/μl (median, 218; IQR, 179 to 260), respectively], indicating early- or late-stage disease progression [noncontroller/high CD4 (n = 14) or noncontroller/low CD4 (n = 14)]. We also identified subjects with undetectable viral loads on antiretroviral therapy ("Suppressed," n = 14) with CD4 counts of >500 cells/μl (median, 720; IQR, 658 to 830) and a high-risk HIV-seronegative group (Negative, n = 14) (CD4 counts not determined).

Study C. For the longitudinal analysis of acutely infected subjects shown in Fig. 3E, cryopreserved PBMCs were obtained from 27 participants of the Options Cohort at two time points after infection. The first time point was selected during early infection (acute) at ~3 months after the estimated infection date (median, 3.03; IQR, 2.4 to 3.6) and the second time point at ~12 months of infection (median, 11.6; IQR, 9.1 to 14.3), a time when viral and immunological set

points are established (chronic). We further subdivided these subjects into three groups (Groups 1 to 3) on the basis of previous results demonstrating that both high viral load and high T cell immune activation set points are independent predictors of more rapid $CD4^+$ T cell decline and disease progression (*5*). As illustrated in Fig. 3E, we selected three groups of subjects at the chronic time point based on plasma HIV RNA concentrations (viral load) and T cell immune activation [measured by the median fluorescence intensity (MdFI) of CD38 on total $CD8^+$ T cells (Fig. 3E, left)]: Group 1 had low viral load (<10,000 copies/ml) and low immune activation, Group 2 had high viral load (>10,000 copies/ml) and high immune activation, and Group 3 had high viral load (>10,000 copies/ml) but low immune activation. Groups 2 and 3 had no significant differences in viral load, and Groups 1 and 2 had no significant differences in immune activation ($P > 0.1$, Mann-Whitney). Conversely, Groups 2 and 3 had significantly higher viral load than Group 1, and Group 2 had significantly higher immune activation than Groups 1 and 3 ($P < 0.05$, Mann-Whitney). This strategy was designed to select subjects who would show different rates of CD4 decline in the absence of antiretroviral treatment, with Group 2 subjects predicted to be more rapid progressors than those in Groups 1 and 3.

Study D. For the simultaneous analysis of T_H17 and T_{reg} cells in specimens of PBMCs and rectosigmoid biopsy tissue (Fig. 4) as well as for analysis of mRNA by PCR (Fig. 2A), immunohistochemistry (Fig. 2B), and 16*S* rDNA (Fig. 4A), paired rectosigmoid biopsies and blood samples were obtained from subjects in the SCOPE Cohort who were (i) noncontrollers ($n = 11$), defined as untreated individuals with plasma HIV RNA concentrations of >10,000 copies/ml (median, 24,734; range, 15,534 to 91,199) and $CD4^+$ T cell counts of ≥200 cells/μl (median, 253; range, 196 to 673), and (ii) controllers ($n = 9$), defined as untreated individuals with undetectable (<75 RNA copies/ml) or plasma HIV RNA concentrations of <2000 RNA copies/ml (median, 77; range, <75 to 1957) and $CD4^+$ T cell counts of ≥500 cells/μl (median, 701; range, 518 to 1507).

All cryopreserved samples were obtained after density centrifugation of acid citrate dextrose (ACD) solution–treated collection tubes following standard procedures. All samples in Studies B and C were thawed, processed, and analyzed at the same time to limit technical variations during processing and flow cytometry measurements. All data from Studies A to D were processed and analyzed in a blinded fashion.

Tissue collection and processing

Whole blood was collected into EDTA-containing tubes (BD Biosciences) for cell counts and into ACD-containing tubes (BD Biosciences) for purification of plasma and PBMCs. All HIV-infected participants in Study D underwent paired blood draw (except one) and flexible sigmoidoscopy. The sigmoidoscope was advanced to the rectosigmoid region, and 30 mucosal biopsies were obtained in a circumferential fashion at ~15 cm from the anal verge using a disposable biopsy forceps with a 3.3-mm outside diameter. Focal areas with visible evidence of inflammation were avoided. For each participant, 4 biopsy specimens were fixed in buffered formalin and paraffin embedded (for immunohistochemistry), 2 biopsies were immediately frozen in optimal cutting temperature buffer and transferred to a −80°C freezer, 4 biopsies were placed in RNAlater (Ambion) (for RNA extraction), and the remaining 20 biopsy specimens were placed in 15 ml of R-10 [RPMI 1640 medium (Invitrogen) supplemented with 10% fetal calf serum (FCS) (Hyclone) and 50 U/50 μg of penicillin-streptomycin per milliliter] and transported within 2 hours to the laboratory for immediate processing. A suspension of mucosal cells from rectosigmoid biopsies was obtained after mechanical digestion and then three successive collagenase type II treatments (0.5 mg/ml) (Sigma-Aldrich). Cell viability in all samples was assessed by trypan blue exclusion. After purification, PBMCs and rectosigmoid biopsy cells were counted and resuspended at 3×10^6 to 8×10^6 cells/ml for subsequent phenotyping and functional analysis in R-10 medium [RPMI 1640 medium supplemented with 10% FCS, 10 mM Hepes, 2 mM L-glutamine, penicillin-streptomycin (50 U/50 μg ml^{-1}), and 0.1 mM Gibco minimum essential medium nonessential amino acid solution (all from Invitrogen)].

Measurement of tryptophan and kynurenine concentrations in plasma

Tryptophan and kynurenine concentrations in plasma were measured by high-performance liquid chromatography. In brief, 100 μl of plasma was combined with 100 μl of 3-nitro-tyrosine (5 μg/ml), which served as an internal standard. Tricholoroacetic acid (25 μl) (20%) was then added to precipitate all proteins, and the sample was centrifuged and ~100 μl of the supernatant was collected for analysis. From the supernatant, 20 μl of sample was injected into the column [Nova-Pak C18 30 cm × 3.1 mm (Waters)] and run through in mobile phase [15 mM potassium phosphate (diacid) (pH 7.0), with 2.75% acetonitrile]. Tryptophan concentrations were measured by fluorescence (Shimadzu RF 530 fluorescence detector: excitation, 285 nM; detection, 365 nM), and kynurenine concentrations were measured with an ultraviolet detector (Waters M486 UV detector: detection, 360 nM). Standard curves and quality control samples [phosphate-buffered saline–bovine serum albumin (BSA) (5%) with 50 μM tryptophan and 2.5 μM kynurenine] were included in each run, and final concentrations were determined based on internal standards and standard curves.

In cell culture supernatants, tryptophan and kynurenine concentrations were measured instead by liquid chromatography–tandem mass spectrometry (LC-MS/MS). The plasma sample (100 μl) was added to 100 μl of internal standard, 3-nitro-tyrosine (5 μg/ml), and vortexed for 1 min, and 20 μl of trifluoroacetic acid was added to precipitate the proteins. After vortexing for 1 min, the mixture was centrifuged at 3000 rpm for 10 min. The supernatant was transferred to autosampler vial, and 5 μl was injected to the LC-MS/MS system. The mass detector was a Micromass Quattro Ultima using electrospray positive ionization mode. The multiple reaction monitor was set at 205.1 to 188.0 mass/charge ratio (*m/z*) for Trp, 209.1 to 192.0 *m/z* for kynurenine, and 227.0 to 181.1 *m/z* for internal standard, respectively. The column was Synergi Polar RP (4.6 × 75 mm, 4-μm particle size) with mobile phase consisting of 2% acetonitrile, 5.4% methanol, and 0.1% formic acid. The flow rate was 1.0 ml/min, one-fourth split into the mass system. The standard curve was generated by adding tryptophan and kynurenine standard solutions to water and treated in the same way as the plasma sample.

Immunohistochemistry and immunofluorescence

IDO1 expression was measured by immunohistochemistry and immunofluorescence with a rabbit polyclonal antibody that was prepared as described (*60*). Lymphoid tissues and rectal biopsies were fixed in formalin (10% normal buffered formalin) and embedded in paraffin, and 5-μm-thick sections were prepared for staining. Tissue sections were

rehydrated and incubated in a pressure cooker with sodium citrate buffer for antigen retrieval. For both immunohistochemistry and immunofluorescence, sections were incubated for 1 hour with a polyclonal antibody to IDO1 (2 μg/ml) in tris-buffered saline–BSA (2%). For immunohistochemistry, detection of primary antibodies was performed with horseradish peroxidase polymer (DAKO Envision kit)–conjugated antibodies to rabbit and developed with 3,3′-diaminobenzidine. Counterstains were done with Mayer's hematoxylin. For immunofluorescence staining, sections were washed and incubated for 1 hour with Alexa Fluor 488 (Invitrogen) fluorophore–conjugated secondary antibodies to rabbit. Staining for DEC205 was performed using a mouse monoclonal antibody to DEC205 (NCL-L-DEC205; Novocastra) followed by Alexa Fluor 555–conjugated secondary antibody to mouse (Invitrogen). The nuclear stain 4′,6-diamidino-2-phenylindole (Sigma-Aldrich) was used as a counterstain for immunofluorescence microscopy.

Detection of plasma sCD14, EndoCAb, and LPS concentrations and quantification of 16*S* rDNA and IDO1 mRNA

Measurement of plasma sCD14, EndoCAb, and LPS was performed as described (*28*). 16*S* rDNA and IDO1 mRNA were measured by quantitative real-time PCR (RT-PCR) on stored plasma samples. DNA was isolated from 200 μl of plasma with Qiagen DNeasy Blood kit according to the manufacturer's instructions. Quantitative PCR for measurement of bacterial 16*S* rDNA was carried out according to the methods outlined in (*61*). Measurement of IDO1 transcript was performed by RT-PCR on RNA from rectal biopsies isolated by phenol-chloroform extraction (TRIzol) (Invitrogen) after reverse transcription (Invitrogen). For RT-PCR analysis, 1 μg of RNA from each sample was reverse-transcribed in a 20-μl reaction with SuperScript III (Invitrogen). The RT reaction was further diluted 1:5, and 1 μl of the resulting cDNA was used in quantitative RT-PCR reactions with labeling of fluorescent double-stranded DNA dye by SYBR Green with primers (IDO forward: 5′-GGCAAAGGTCATGGAGATGT-3′; and IDO reverse: 5′-CTGCAGTCTCCATCACGAAA-3′) designed in house that span introns to avoid amplification of genomic DNA. All values were normalized to β-actin values

Preparation and stimulation of human DCs

Human DCs were generated from $CD14^+$ monocytes purified from whole PBMCs by positive selection for $CD14^+$ cells (Miltenyi). The purified $CD14^+$ cells were cultured in serum-free medium (XVIVO20; Lonza) in the presence of granulocyte-monocyte colony-stimulating factor (10 ng/ml) and IL-4 (10 ng/ml) for 6 days. Cytokines and growth factors were added on days 0, 2, and 4. On the final day of culture, the DCs were treated with various cytokines or TLR agonists. Supernatants were isolated 48 hours later, and kynurenine and tryptophan concentrations were measured as described above.

Flow cytometry on peripheral blood and rectal biopsies

Panels of antibodies used for phenotypic detection and intracellular cytokine detection are described in table S2. Cytokine assays were performed in vitro on 5×10^5 cells after no stimulation or stimulation with media, staphylococcal enterotoxin B (1 μg/ml), or phorbol 12-myristate 13-acetate (PMA) (10 ng/ml) and ionomycin (1 μg/ml) for 6 hours at 37°C in the presence of brefeldin A (GolgiPlug, BD Pharmingen). Cytokine detection and phenotyping were performed by cell surface staining and subsequent intracellular staining following the manufacturer's instructions [BD or eBioscience (T_{reg} Panel 2)]. Cytokine analysis was performed after stringent gating on singlet live ($AQUA^-$) $CD4^+$ or $CD8^+$ T cell lymphocytes from rectosigmoid cells or from PBMCs and reported as background-subtracted values from the unstimulated cell population from each patient and for each stimulus, as described (*62*). Notably, whenever possible, we used the MdFI of CD38 on $CD8^+$ T cells as the reference marker for T cell immune activation, as described (*5*). However, when CD38 MdFI measurements were not possible (for example, at a time when samples were not analyzed together), the frequency of $CD8^+$ T cells that were gated positive for CD38 was used instead. Fluorescence-activated cell sorting (FACS) analysis was performed on a four-laser BD LSR-II flow cytometers using High Throughput System plate readers (BD Biosciences). Data were analyzed with FlowJo software v6-8 (Treestar) and transferred into analysis and graphic software including Excel (Windows), StatView (Abacus Concepts), SPICE (provided by M. Roederer), and/or GraphPad Prism4.

In vitro T cell activation assays

PBMCs were isolated from healthy volunteers by centrifugation of whole blood over Ficoll-Hypaque density gradients and washed in freshly prepared R-10. The cells were subsequently labeled with the dye CFSE (Invitrogen) and cultured at a concentration of 3×10^5 cells per well in 96-well U-bottom tissue culture plates that had previously been coated with antibody to CD3 (clone SP34-1; 0.5 μg/ml; BD Pharmingen). Soluble antibody to CD28 (0.5 μg/ml; BD Pharmingen) and irradiated CD3-depleted PBMCs from an unrelated (allogeneic) donor were added to each well at a final concentration of 1×10^5 cells per well. Finally, graded concentrations of different tryptophan catabolites or vehicle (dimethyl sulfoxide) were added to the wells and the cells were cultured for 6 days at 37°C. Tryptophan catabolites (or vehicle controls) were replaced on day 3 in 100 μl of fresh RPMI 1640 culture medium. For detection of cytokine production by flow cytometry, the cells were stimulated on day 6 for 5 hours at 37°C with PMA (10 ng/ml) and ionomycin (1 μg/ml) in the presence of brefeldin A (GolgiPlug). Surface staining and intracellular staining were performed as described in the previous section. For FoxP3 staining, cells were harvested on day 6 and stained as described in the previous section. Notably, donor-to-donor variability was observed in the percentage of change in the T_H1 population in response to 3-HAA, with some subjects showing increases and others decreases (or no change) in the fraction of T_H1 cells.

Statistical analysis

The Mann-Whitney *U* test was used for group comparisons. In the Options Cohort (Study C), mixed-effects longitudinal statistical models were used to test the impact of peripheral memory T_H17 cells, blood $CD4^+$ T cell counts, and viral load on $CD8^+$ T cell activation levels (%Ki67) during the 3- to 12-month time period after the estimated date of HIV infection. These models were run in the SAS System 9.2 and specified random effects for time and the individual. The Spearman rank correlation test was used to determine correlations between variables, with R_s being the Spearman correlation coefficient. *P* values of <0.05 were considered statistically significant.

SUPPLEMENTARY MATERIAL

www.sciencetranslationalmedicine.org/cgi/content/full/2/32/32ra36/DC1

Fig. S1. Characterization of IDO up-regulation in mDCs from HIV^+ subjects.

Fig. S2. IDO activity on mDCs in vitro with combined IL-17 and/or IL-1β–IL-6–TNFα.

Fig. S3. Characterization of T_H17 memory phenotype in PBMCs and in rectosigmoid biopsies.
Fig. S4. IDO catabolites affect T_H17 cells in PBMCs from healthy donors and HIV-infected subjects.
Table S1. Individual characteristic of subjects.
Table S2. Antibody panels for multiparameter flow cytometry.

REFERENCES AND NOTES

1. D. C. Douek, M. Roederer, R. A. Koup, Emerging concepts in the immunopathogenesis of AIDS. *Annu. Rev. Med.* **60**, 471–484 (2009).
2. J. M. McCune, The dynamics of $CD4^+$ T-cell depletion in HIV disease. *Nature* **410**, 974–979 (2001).
3. H. Valdez, M. M. Lederman, Cytokines and cytokine therapies in HIV infection. *AIDS Clin. Rev.* 187–228 (1997).
4. M. F. Murray, Tryptophan depletion and HIV infection: A metabolic link to pathogenesis. *Lancet Infect. Dis.* **3**, 644–652 (2003).
5. S. G. Deeks, C. M. Kitchen, L. Liu, H. Guo, R. Gascon, A. B. Narváez, P. Hunt, J. N. Martin, J. O. Kahn, J. Levy, M. S. McGrath, F. M. Hecht, Immune activation set point during early HIV infection predicts subsequent $CD4^+$ T-cell changes independent of viral load. *Blood* **104**, 942–947 (2004).
6. L. H. Kuller, R. Tracy, W. Belloso, S. De Wit, F. Drummond, H. C. Lane, B. Ledergerber, J. Lundgren, J. Neuhaus, D. Nixon, N. I. Paton, J. D. Neaton; INSIGHT SMART Study Group, Inflammatory and coagulation biomarkers and mortality in patients with HIV infection. *PLoS Med.* **5**, e203 (2008).
7. A. L. Mellor, D. H. Munn, IDO expression by dendritic cells: Tolerance and tryptophan catabolism. *Nat. Rev. Immunol.* **4**, 762–774 (2004).
8. H. J. Ball, H. J. Yuasa, C. J. Austin, S. Weiser, N. H. Hunt, Indoleamine 2,3-dioxygenase-2; a new enzyme in the kynurenine pathway. *Int. J. Biochem. Cell Biol.* **41**, 467–471 (2009).
9. M. Platten, P. P. Ho, S. Youssef, P. Fontoura, H. Garren, E. M. Hur, R. Gupta, L. Y. Lee, B. A. Kidd, W. H. Robinson, R. A. Sobel, M. L. Selley, L. Steinman, Treatment of autoimmune neuroinflammation with a synthetic tryptophan metabolite. *Science* **310**, 850–855 (2005).
10. T. M. Bauer, L. P. Jiga, J. J. Chuang, M. Randazzo, G. Opelz, P. Terness, Studying the immunosuppressive role of indoleamine 2,3-dioxygenase: Tryptophan metabolites suppress rat allogeneic T-cell responses in vitro and in vivo. *Transpl. Int.* **18**, 95–100 (2005).
11. D. Fuchs, A. A. Möller, G. Reibnegger, E. R. Werner, G. Werner-Felmayer, M. P. Dierich, H. Wachter, Increased endogenous interferon-γ and neopterin correlate with increased degradation of tryptophan in human immunodeficiency virus type 1 infection. *Immunol. Lett.* **28**, 207–211 (1991).
12. J. B. Katz, A. J. Muller, G. C. Prendergast, Indoleamine 2,3-dioxygenase in T-cell tolerance and tumoral immune escape. *Immunol. Rev.* **222**, 206–221 (2008).
13. D. H. Munn, M. Zhou, J. T. Attwood, I. Bondarev, S. J. Conway, B. Marshall, C. Brown, A. L. Mellor, Prevention of allogeneic fetal rejection by tryptophan catabolism. *Science* **281**, 1191–1193 (1998).
14. D. H. Munn, M. D. Sharma, B. Baban, H. P. Harding, Y. Zhang, D. Ron, A. L. Mellor, GCN2 kinase in T cells mediates proliferative arrest and anergy induction in response to indoleamine 2,3-dioxygenase. *Immunity* **22**, 633–642 (2005).
15. P. Terness, T. M. Bauer, L. Röse, C. Dufter, A. Watzlik, H. Simon, G. Opelz, Inhibition of allogeneic T cell proliferation by indoleamine 2,3-dioxygenase-expressing dendritic cells: Mediation of suppression by tryptophan metabolites. *J. Exp. Med.* **196**, 447–457 (2002).
16. T. Korn, E. Bettelli, M. Oukka, V. K. Kuchroo, IL-17 and Th17 cells. *Annu. Rev. Immunol.* **27**, 485–517 (2009).
17. K. H. Mills, Induction, function and regulation of IL-17-producing T cells. *Eur. J. Immunol.* **38**, 2636–2649 (2008).
18. D. Favre, S. Lederer, B. Kanwar, Z. M. Ma, S. Proll, Z. Kasakow, J. Mold, L. Swainson, J. D. Barbour, C. R. Baskin, R. Palermo, I. Pandrea, C. J. Miller, M. G. Katze, J. M. McCune, Critical loss of the balance between Th17 and T regulatory cell populations in pathogenic SIV infection. *PLoS Pathog.* **5**, e1000295 (2009).
19. J. M. Brenchley, M. Paiardini, K. S. Knox, A. I. Asher, B. Cervasi, T. E. Asher, P. Scheinberg, D. A. Price, C. A. Hage, L. M. Kholi, A. Khoruts, I. Frank, J. Else, T. Schacker, G. Silvestri, D. C. Douek, Differential Th17 CD4 T-cell depletion in pathogenic and nonpathogenic lentiviral infections. *Blood* **112**, 2826–2835 (2008).
20. A. De Luca, C. Montagnoli, T. Zelante, P. Bonifazi, S. Bozza, S. Moretti, C. D'Angelo, C. Vacca, L. Boon, F. Bistoni, P. Puccetti, F. Fallarino, L. Romani, Functional yet balanced reactivity to *Candida albicans* requires TRIF, MyD88, and IDO-dependent inhibition of *Rorc*. *J. Immunol.* **179**, 5999–6008 (2007).
21. L. Romani, F. Fallarino, A. De Luca, C. Montagnoli, C. D'Angelo, T. Zelante, C. Vacca, F. Bistoni, M. C. Fioretti, U. Grohmann, B. H. Segal, P. Puccetti, Defective tryptophan catabolism underlies inflammation in mouse chronic granulomatous disease. *Nature* **451**, 211–215 (2008).
22. M. Huengsberg, J. B. Winer, M. Gompels, R. Round, J. Ross, M. Shahmanesh, Serum kynurenine-to-tryptophan ratio increases with progressive disease in HIV-infected patients. *Clin. Chem.* **44**, 858–862 (1998).
23. J. D. Estes, Q. Li, M. R. Reynolds, S. Wietgrefe, L. Duan, T. Schacker, L. J. Picker, D. I. Watkins, J. D. Lifson, C. Reilly, J. Carlis, A. T. Haase, Premature induction of an immunosuppressive regulatory T cell response during acute simian immunodeficiency virus infection. *J. Infect. Dis.* **193**, 703–712 (2006).
24. A. Boasso, J. P. Herbeuval, A. W. Hardy, S. A. Anderson, M. J. Dolan, D. Fuchs, G. M. Shearer, HIV inhibits $CD4^+$ T-cell proliferation by inducing indoleamine 2,3-dioxygenase in plasmacytoid dendritic cells. *Blood* **109**, 3351–3359 (2007).
25. B. Malleret, B. Manéglier, I. Karlsson, P. Lebon, M. Nascimbeni, L. Perié, P. Brochard, B. Delache, J. Calvo, T. Andrieu, O. Spreux-Varoquaux, A. Hosmalin, R. Le Grand, B. Vaslin, Primary infection with simian immunodeficiency virus: Plasmacytoid dendritic cell homing to lymph nodes, type I interferon, and immune suppression. *Blood* **112**, 4598–4608 (2008).
26. A. S. Beignon, K. McKenna, M. Skoberne, O. Manches, I. DaSilva, D. G. Kavanagh, M. Larsson, R. J. Gorelick, J. D. Lifson, N. Bhardwaj, Endocytosis of HIV-1 activates plasmacytoid dendritic cells via Toll-like receptor–viral RNA interactions. *J. Clin. Invest.* **115**, 3265–3275 (2005).
27. N. Kadowaki, The divergence and interplay between pDC and mDC in humans. *Front. Biosci.* **14**, 808–817 (2009).
28. J. M. Brenchley, D. A. Price, T. W. Schacker, T. E. Asher, G. Silvestri, S. Rao, Z. Kazzaz, E. Bornstein, O. Lambotte, D. Altmann, B. R. Blazar, B. Rodriguez, L. Teixeira-Johnson, A. Landay, J. N. Martin, F. M. Hecht, L. J. Picker, M. M. Lederman, S. G. Deeks, D. C. Douek, Microbial translocation is a cause of systemic immune activation in chronic HIV infection. *Nat. Med.* **12**, 1365–1371 (2006).
29. R. Yoshida, O. Hayaishi, Induction of pulmonary indoleamine 2,3-dioxygenase by intraperitoneal injection of bacterial lipopolysaccharide. *Proc. Natl. Acad. Sci. U.S.A.* **75**, 3998–4000 (1978).
30. R. Yoshida, J. Imanishi, T. Oku, T. Kishida, O. Hayaishi, Induction of pulmonary indoleamine 2,3-dioxygenase by interferon. *Proc. Natl. Acad. Sci. U.S.A.* **78**, 129–132 (1981).
31. M. W. Taylor, G. S. Feng, Relationship between interferon-γ, indoleamine 2,3-dioxygenase, and tryptophan catabolism. *FASEB J.* **5**, 2516–2522 (1991).
32. J. M. Brenchley, D. A. Price, D. C. Douek, HIV disease: Fallout from a mucosal catastrophe? *Nat. Immunol.* **7**, 235–239 (2006).
33. I. V. Pandrea, R. Gautam, R. M. Ribeiro, J. M. Brenchley, I. F. Butler, M. Pattison, T. Rasmussen, P. A. Marx, G. Silvestri, A. A. Lackner, A. S. Perelson, D. C. Douek, R. S. Veazey, C. Apetrei, Acute loss of intestinal $CD4^+$ T cells is not predictive of simian immunodeficiency virus virulence. *J. Immunol.* **179**, 3035–3046 (2007).
34. M. Raffatellu, R. L. Santos, D. E. Verhoeven, M. D. George, R. P. Wilson, S. E. Winter, I. Godinez, S. Sankaran, T. A. Paixao, M. A. Gordon, J. K. Kolls, S. Dandekar, A. J. Bäumler, Simian immunodeficiency virus–induced mucosal interleukin-17 deficiency promotes *Salmonella* dissemination from the gut. *Nat. Med.* **14**, 421–428 (2008).
35. E. Bettelli, Y. Carrier, W. Gao, T. Korn, T. B. Strom, M. Oukka, H. L. Weiner, V. K. Kuchroo, Reciprocal developmental pathways for the generation of pathogenic effector T_H17 and regulatory T cells. *Nature* **441**, 235–238 (2006).
36. D. Mucida, Y. Park, G. Kim, O. Turovskaya, I. Scott, M. Kronenberg, H. Cheroutre, Reciprocal T_H17 and regulatory T cell differentiation mediated by retinoic acid. *Science* **317**, 256–260 (2007).
37. L. Zhou, J. E. Lopes, M. M. Chong, I. I. Ivanov, R. Min, G. D. Victora, Y. Shen, J. Du, Y. P. Rubtsov, A. Y. Rudensky, S. F. Ziegler, D. R. Littman, TGF-β-induced Foxp3 inhibits T_H17 cell differentiation by antagonizing RORγt function. *Nature* **453**, 236–240 (2008).
38. F. J. Quintana, A. S. Basso, A. H. Iglesias, T. Korn, M. F. Farez, E. Bettelli, M. Caccamo, M. Oukka, H. L. Weiner, Control of T_{reg} and T_H17 cell differentiation by the aryl hydrocarbon receptor. *Nature* **453**, 65–71 (2008).
39. O. Manches, D. Munn, A. Fallahi, J. Lifson, L. Chaperot, J. Plumas, N. Bhardwaj, HIV-activated human plasmacytoid DCs induce T_{regs} through an indoleamine 2,3-dioxygenase–dependent mechanism. *J. Clin. Invest.* **118**, 3431–3439 (2008).
40. M. Yoshioka, W. G. Bradley, P. Shapshak, I. Nagano, R. V. Stewart, K. Q. Xin, A. K. Srivastava, S. Nakamura, Role of immune activation and cytokine expression in HIV-1-associated neurologic diseases. *Adv. Neuroimmunol.* **5**, 335–358 (1995).
41. X. Dai, B. T. Zhu, Suppression of T-cell response and prolongation of allograft survival in a rat model by tryptophan catabolites. *Eur. J. Pharmacol.* **606**, 225–232 (2009).
42. A. S. Basso, H. Cheroutre, D. Mucida, More stories on Th17 cells. *Cell Res.* **19**, 399–411 (2009).
43. H. D. Ochs, M. Oukka, T. R. Torgerson, T_H17 cells and regulatory T cells in primary immunodeficiency diseases. *J. Allergy Clin. Immunol.* **123**, 977–983 (2009).
44. B. Kanwar, D. Favre, J. M. McCune, Th17 and regulatory T cells: Implications for AIDS pathogenesis. *Curr. Opin. HIV AIDS* **5**, 151–157 (2010).
45. D. R. Littman, A. Y. Rudensky, Th17 and regulatory T cells in mediating and restraining inflammation. *Cell* **140**, 845–858 (2010).
46. J. Furuzawa-Carballeda, M. I. Vargas-Rojas, A. R. Cabral, Autoimmune inflammation from the Th17 perspective. *Autoimmun. Rev.* **6**, 169–175 (2007).
47. W. Ouyang, J. K. Kolls, Y. Zheng, The biological functions of T helper 17 cell effector cytokines in inflammation. *Immunity* **28**, 454–467 (2008).
48. I. I. Ivanov, B. S. McKenzie, L. Zhou, C. E. Tadokoro, A. Lepelley, J. J. Lafaille, D. J. Cua, D. R. Littman, The orphan nuclear receptor RORγt directs the differentiation program of proinflammatory $IL-17^+$ T helper cells. *Cell* **126**, 1121–1133 (2006).

49. M. S. Sundrud, S. B. Koralov, M. Feuerer, D. P. Calado, A. E. Kozhaya, A. Rhule-Smith, R. E. Lefebvre, D. Unutmaz, R. Mazitschek, H. Waldner, M. Whitman, T. Keller, A. Rao, Halofuginone inhibits T_H17 cell differentiation by activating the amino acid starvation response. *Science* **324**, 1334–1338 (2009).
50. M. D. Sharma, D. Y. Hou, Y. Liu, P. A. Koni, R. Metz, P. Chandler, A. L. Mellor, Y. He, D. H. Munn, Indoleamine 2,3-dioxygenase controls conversion of $Foxp3^+$ T_{regs} to TH17-like cells in tumor-draining lymph nodes. *Blood* **113**, 6102–6111 (2009).
51. H. W. Virgin, E. J. Wherry, R. Ahmed, Redefining chronic viral infection. *Cell* **138**, 30–50 (2009).
52. E. Traub, Epidemiology of lymphocytic choriomeningitis in a mouse stock observed for four years. *J. Exp. Med.* **69**, 801–817 (1939).
53. A. M. Silverstein, Ontogeny of the immune response. *Science* **144**, 1423–1428 (1964).
54. D. L. Sodora, J. S. Allan, C. Apetrei, J. M. Brenchley, D. C. Douek, J. G. Else, J. D. Estes, B. H. Hahn, V. M. Hirsch, A. Kaur, F. Kirchhoff, M. Muller-Trutwin, I. Pandrea, J. E. Schmitz, G. Silvestri, Toward an AIDS vaccine: Lessons from natural simian immunodeficiency virus infections of African nonhuman primate hosts. *Nat. Med.* **15**, 861–865 (2009).
55. Y. A. Taher, B. J. Piavaux, R. Gras, B. C. van Esch, G. A. Hofman, N. Bloksma, P. A. Henricks, A. J. van Oosterhout, Indoleamine 2,3-dioxygenase–dependent tryptophan metabolites contribute to tolerance induction during allergen immunotherapy in a mouse model. *J. Allergy Clin. Immunol.* **121**, 983–991.e2 (2008).
56. G. J. Gurtner, R. D. Newberry, S. R. Schloemann, K. G. McDonald, W. F. Stenson, Inhibition of indoleamine 2,3-dioxygenase augments trinitrobenzene sulfonic acid colitis in mice. *Gastroenterology* **125**, 1762–1773 (2003).
57. T. Hayashi, J. H. Mo, X. Gong, C. Rossetto, A. Jang, L. Beck, G. I. Elliott, I. Kufareva, R. Abagyan, D. H. Broide, J. Lee, E. Raz, 3-Hydroxyanthranilic acid inhibits PDK1 activation and suppresses experimental asthma by inducing T cell apoptosis. *Proc. Natl. Acad. Sci. U.S.A.* **104**, 18619–18624 (2007).
58. A. Boasso, M. Vaccari, D. Fuchs, A. W. Hardy, W. P. Tsai, E. Tryniszewska, G. M. Shearer, G. Franchini, Combined effect of antiretroviral therapy and blockade of IDO in SIV-infected rhesus macaques. *J. Immunol.* **182**, 4313–4320 (2009).
59. R. Potula, L. Poluektova, B. Knipe, J. Chrastil, D. Heilman, H. Dou, O. Takikawa, D. H. Munn, H. E. Gendelman, Y. Persidsky, Inhibition of indoleamine 2,3-dioxygenase (IDO) enhances elimination of virus-infected macrophages in an animal model of HIV-1 encephalitis. *Blood* **106**, 2382–2390 (2005).
60. D. H. Munn, M. D. Sharma, J. R. Lee, K. G. Jhaver, T. S. Johnson, D. B. Keskin, B. Marshall, P. Chandler, S. J. Antonia, R. Burgess, C. L. Slingluff Jr., A. L. Mellor, Potential regulatory function of human dendritic cells expressing indoleamine 2,3-dioxygenase. *Science* **297**, 1867–1870 (2002).
61. W. Jiang, M. M. Lederman, P. Hunt, S. F. Sieg, K. Haley, B. Rodriguez, A. Landay, J. Martin, E. Sinclair, A. I. Asher, S. G. Deeks, D. C. Douek, J. M. Brenchley, Plasma levels of bacterial DNA correlate with immune activation and the magnitude of immune restoration in persons with antiretroviral-treated HIV infection. *J. Infect. Dis.* **199**, 1177–1185 (2009).
62. P. Loke, D. Favre, P. W. Hunt, J. M. Leung, B. Kanwar, J. N. Martin, S. G. Deeks, J. M. McCune, Correlating cellular and molecular signatures of mucosal immunity that distinguish HIV controllers from noncontrollers. *Blood* **115**, e20–e32 (2010).

63. **Acknowledgments:** We thank P. Lizak for technical support, H. Yee and M. Somsouk for assistance in obtaining rectosigmoid biopsies, W. Jiang for help with the assay for 16*S* rDNA, K. A. Reimann for providing antibodies through the NIH Reagent Resource Program, and M. Roederer for providing the SPICE software. **Funding:** These studies were supported in part by R37 AI40312 and DPI OD00329 (J.M.M.), Elizabeth Glaser Pediatric AIDS Foundation 77510-29 (D.F.), R01 K23 AI065244 (P.W.H.), R01 AI066917 (J.D.B.), P30 AI022763 (F.A.), the intramural research program at National Institute of Allergy and Infectious Diseases–NIH (J.M.B. and D.C.D.), P30 AI27763 (J.N.M. and S.G.D.), and the Harvey V. Berneking Living Trust. The clinical SCOPE cohorts (J.N.M. and S.G.D.) were supported by grants from the NIH (AI069994), the UCSF–GIVI Center for AIDS Research (P30 MH59037), and the UCSF Clinical and Translational Research Institute Clinical Research Center (UL1 RR024131). The Options project was supported by a grant from the NIH to F.M.H. (P01 AI071713). J.M.M. is a recipient of the NIH Director's Pioneer Award Program, part of the NIH Roadmap for Medical Research, through grant DPI OD00329. **Author contributions:** D.F. designed the study; performed experiments in Figs. 3 and 4; provided protocol development, sample, and analysis in Figs. 2 and 5; and wrote the paper. J.M. designed the study and performed experiments in Figs. 1, 2, and 5 and wrote the paper. P.W.H. was involved in study design, recruited subjects, and organized rectosigmoid specimen collection. B.K. prepared rectosigmoid biopsies. P.L. performed IDO mRNA measurements. L.S. performed 16*S* rDNA measurements in Study D. J.D.B. performed multivariate statistical analysis in Study C. M.M.L. participated in experiment in fig. S4B. A.J., F.A., and Y.H. provided kynurenine and tryptophan measurements or technology in Study A and B. D.C.D. and J.M.B. provided LPS, sCD14, and EndoCAb measurements in Study A. J.N.M. was involved in subject recruitment, specimen collection, and data management in Study A, B, and D (SCOPE cohort). F.M.H. was involved in study design and subject recruitment in Study C (Options cohort). S.G.D. was involved in study design, subject recruitment (SCOPE cohort), specimen collection, and editing the paper. J.M.M. designed the study, provided the funding, and wrote the paper. **Competing interests:** The authors report no competing interests.

Submitted 13 November 2009
Accepted 30 April 2010
Published 19 May 2010
10.1126/scitranslmed.3000632

Citation: D. Favre, J. Mold, P. W. Hunt, B. Kanwar, P. Loke, L. Seu, J. D. Barbour, M. M. Lowe, A. Jayawardene, F. Aweeka, Y. Huang, D. C. Douek, J. M. Brenchley, J. N. Martin, F. M. Hecht, S. G. Deeks, J. M. McCune, Tryptophan catabolism by indoleamine 2,3-dioxygenase 1 alters the balance of T_H17 to regulatory T cells in HIV disease. *Sci. Transl. Med.* **2**, 32ra36 (2010).